EXPERIMENTAL STUDY OF VISCOUS FLOW ON MULTIPLE ELEMENT AIRFOILS

Björn L. G. Ljungström
The Aeronautical Research Institute
of Sweden, FFA

Abstract

The general objectives of high lift development and optimization are first briefly discussed as a background for the experimental efforts. Boundary layer measurements have been carried out on a 2-D high lift wing with a leading edge slat and a single slotted trailing edge flap in order to study the interaction between the different viscous layers involved. Suction is used as a way to vary the conditions for the viscous flow. The effects of viscous interaction on the development of displacement thickness and shape factor are evaluated. It is found that the best high lift performance is obtained when there is only marginal interaction between all the viscous layers. Some boundary layer surveys over double and triple slotted flaps are shown which verify previous assumptions about optimum interaction. The experiments have been compared to calculations with a viscous multiple element method developed by Stevens and Goradia. A few other theoretical methods are commented especially with respect to their representation of viscous interaction.

Notation

U_∞	free-stream velocity
U_o	boundary layer undisturbed velocity
U	boundary layer velocity
U_s	minimum wake velocity
δ^*	boundary layer displacement thickness
θ	momentum loss thickness
$H_{12} = \frac{\delta^*}{\theta}$	shape factor
ℓ	wake transverse length scale
y	wake transverse coordinate
C_w	wall suction reference pressure coefficient $= \frac{p_w - p_{ref}}{q_\infty}$
p_w	wall suction reference pressure
α	angle of attack
L	lift
L/D	lift to drag ratio
C_L	$\frac{L}{\frac{1}{2}\rho U_\infty^2 \cdot S}$ = lift coefficient
$C_{L\ max}$	maximum lift coefficient
C_D	drag coefficient
Re	$\frac{U \cdot C}{\nu}$ = Reynolds number, based on model chord
C	model unextended chord
S	model reference area
δ_s	slat angle
h_s	slat gap
h_{f_1}	first flap gap
h_{f_2}	second flap gap
h_{f_3}	third flap gap

I. Introduction

The design and optimization of high lift systems is one of the critical problems for coming generations of transport aircraft.

Improvements in high lift technology is one possible way to relieve noise and congestion which are now the two major constraints to the further growth of air transportation. The possible utilization of STOL or RTOL aircraft with shorter field lengths and steeper climb and descent-gradients will eventually contribute to achieve this.

High lift development is however also a very practical economical problem for CTOL aircraft development. It is a question of optimizing the payload and range performance for a given field length and also to obtain good mission flexibility which is highly desired by the operators. This does not only concern new aircraft projects. The development of stretched versions of existing aircraft has in several cases been possible due to improved high lift systems (e.g. Boeing 727-300, Fokker F-28 Mk 6000, etc.).

The selection and design of the high lift system for a particular aircraft project becomes particularly difficult due to the large number of other aircraft characteristics that are affected by the high lift system, often in a conflicting way. The most important of these characteristics are:

- Power requirements
- Stability and control
- Cruise performance
- Maintenance requirements
- Structural efficiency, weight
- Noise characteristics
- Ride comfort

The trade off analysis that should hopefully result in an optimum high lift system therefore requires a basic understanding and a reasonable assessment of the complicated interrelations between all these characteristics. Of equal importance is however to choose the appropriate criteria for this optimization. What is it that should be optimized?

The airplane industry and the airlines have traditionally been concerned with the operating costs of the aircraft.

Fig 1 shows suggested trends for DOC (envelopes of best state of the art high lift systems) for a fixed aircraft mission as a function of $C_{L\ max}$.

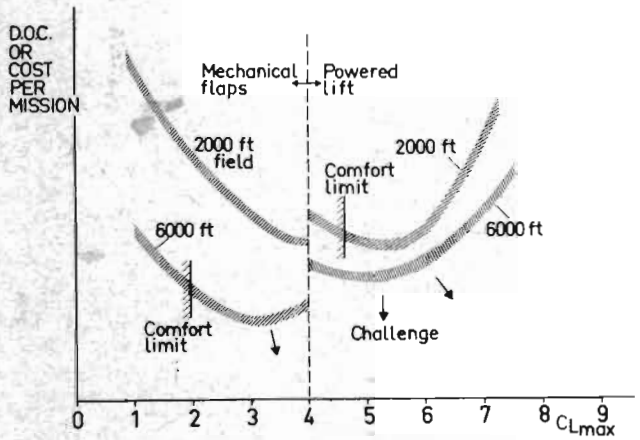

Figure 1. Operating costs v.s. $C_{L\ max}$.

Two different field lengths are plotted. 6000 ft should roughly represent today's medium to short haul aircraft. Each field length exhibits an optimum $C_{L\ max}$ which increases with decreasing field length. The challange to the aerodynamicist is here to try to move these curves downwards, which can be done in many different ways.

The trend for a fixed field length shows first a decreasing cost when the gains in payload to gross weight ratio and cruise performance are greater than the weight and cost penalties of the high lift systems. The optimum is reached when the additional cost and weight of further high lift improvement just balances the improvements in payload and cruise performance.

The trends are interrupted by practical comfort limits in terms of wing loading. These may be somewhat shifted if gust alleviation can be used.

The choice between mechanical and powered lift systems depends on the field length requirement. For any combination of mission requirements and high lift data there is one limiting field length below which powered lift systems become more economical than mechanical ones. The illustrated case shows this to be close to 2000 ft which may be true for some combination of payload, range and cruise speed.

It is however inevitable that costs will always increase with decreasing field length. The DOC figure of merit or even TOC therefore cannot help us to select an optimum combination of field length and high lift performance.

The most important potential benefits and some of the costs due to shorter field lengths do not enter into the DOC or TOC equations. They are felt by the passengers and the general public served by the airline. The passenger is concerned with the total cost and time of a journey from A to B for which air transportation is just one part. He is also concerned with the comfort and general convenience of the service. The general public is concerned with the noise and pollution caused by the aircraft. The criterion from this point of view is therefore quite different from the one shown in Fig 1. It should be composed by total costs divided by total benefits where costs are a combination of total journey cost, noise, pollution and other adverse effects. The benefits are a combination of seat mile production, trip time, and convenience to the traveller.

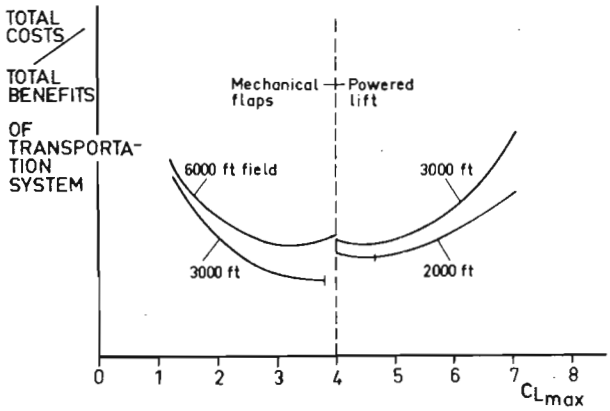

Figure 2. Cost/Benefit of transport system v.s. $C_{L\ max}$.

Fig 2 is drawn to illustrate that the optimum high lift system according to such a criterion may be different from the one in Fig 1. A solution with a higher aircraft operating cost may be a better and more economical solution for the passenger and the general public.

The utilization of shorter field lengths and higher lift coefficients could have the effect to reduce the total trip time for a traveller and possibly also reduce the costs of ground transportation segments of the journey from A to B. This will however also result in increased DOC, changes in noise exposure, pollution and safety both in the air and on the ground. The balance between all these positive and negative effects should give us a useful criterion, that will help us to find an optimum solution. Such a criterion can be used to determine the viability of future STOL operations. The critical factors that will govern the outcome of such a viability study are:

- The assessment of benefits due to short fields as a function of field length and the ability to introduce these benefits into criteria that could initiate and govern STOL system development.
- The development of high lift technology and its effect on cost as a function of field length.
- The development of STOL transport system technology and its possible effect on overall system cost (including improved terminals, navigation and terminal aids, simplified passenger and baggage procedures, etc.).

It is the author's belief that some of the research efforts in high lift technology have been inspired by an overoptimistic assessment of the balance between benefits and costs for STOL operation using sophisticated powered lift systems on 2000 ft runways.

The most cost efficient solution for at least the first generation of STOL is probably an aircraft with mechanical high lift system using 3000 - 4000 ft runways. Improvements of mechanical flaps possibly in combination with gust alleviation systems could reduce this even further down to 2500 ft or so if necessary (see Ref 1).

Fig 3 is intended to illustrate the potential for mechanical flap improvements compared to the best systems that are presently operational. Wind tunnel tests have already demonstrated a 3-dimensional $C_{L\,max}$ of 4.6 for a triple slotted flap on a fairly conventional planform (AR = 8 sweep angle 20°), (Ref 2), which should be compared to 2.9 for Boeing 737.

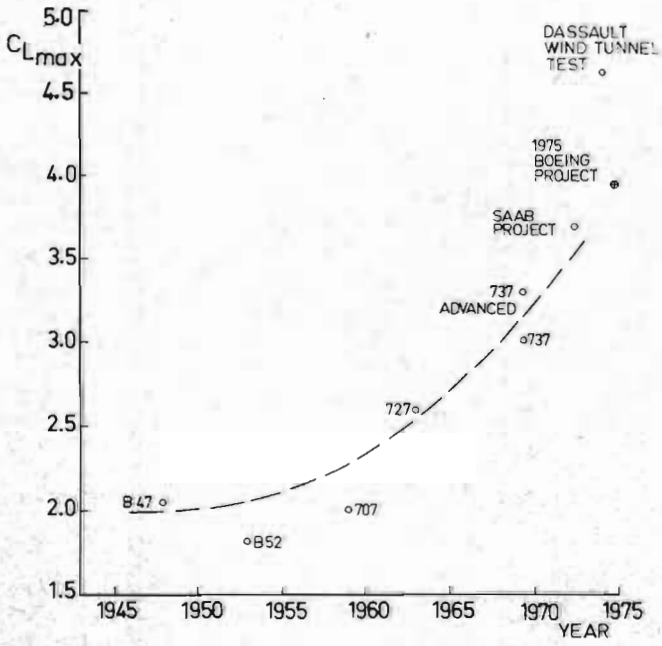

Figure 3. Maximum lift history of mechanical high lift devices.

A high $C_{L\,max}$ alone is certainly not enough to acquire good field performance. The lift to drag ratio is equally important for the take off distance and is also becoming important for the landing case in order to minimize the power setting on approach. High lift research has often been dominated by pure C_L results and discussions. The optimization of L/D for high lift coefficients is therefore an area where there is still room for substantial improvement.

The work discussed in the following is part of a research program which is primarily concerned with development of mechanical flap systems and methods to optimize these. The results concerning boundary layer interactions are however of such a general nature that they should also be of interest for some powered lift applications.

II. Optimization of mechanical flaps

The optimization of a mechanical flap configuration is complicated due to the large number of variables involved. After having selected the number of airfoils elements there still remains a set of 5 independent parameters for each flap element: shape, size, gap, angle, and overlap. A triple slotted configuration with a leading edge slat will consequently have a total of 20 variables. This means that it is virtually impossible to carry out an unconditional experimental program of parameter variations with any hope to reach something optimized within reasonable time.

Present theoretical methods cannot solve this problem for us. A purely theoretical optimization of a high lift geometry would require a calculation method which can predict the growth of all the different viscous layers, their interaction and the onset and spreading of local separations. The best approach under present conditions should therefore be a combination of calculations and experimental parameter variations governed by some understanding of the fundamental characteristics of the flow over multiple element airfoils. Available potential flow calculation methods can be used to choose the geometries that are to be tested experimentally.

The viscous effects due to different parameter variations cannot yet be predicted with sufficient accuracy. There is a definite requirement for more detailed studies of the complicated viscous flow effects and their impact on the optimization of the high lift geometry. Such studies are of importance both for experimental high lift development and as a support to the work on theoretical calculation methods. The 2-D experiments discussed in this paper were conceived as a contribution in both these respects.

2-D testing technique

2-dimensional wind tunnel testing is considered to be a convenient method to study some of the more fundamental aspects of high lift

aerodynamics. The present results are obtained in the 2-D insert test section of the 3.6 m low speed tunnel at FFA (The Aeronautical Research Institute of Sweden). The test section walls are equipped with boundary layer control which is considered an absolute requirement if $C_{L\ max}$ - trends are to be studied. This is illustrated in Fig 4, which shows C_L-α curves for varying wall suction pressure.

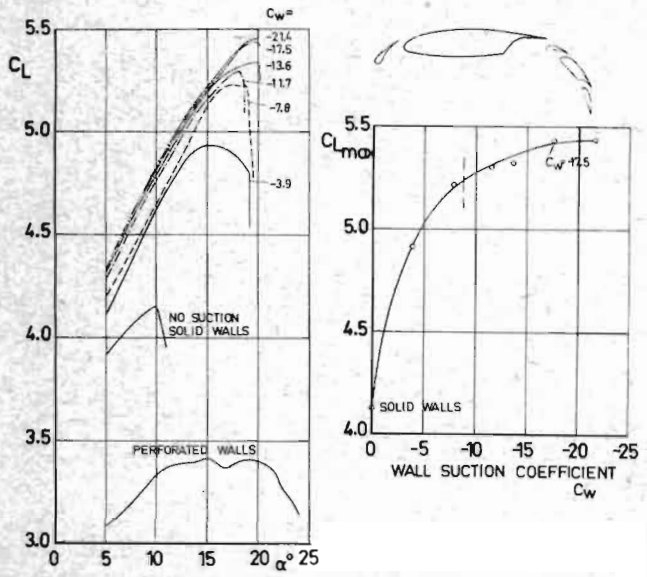

Figure 4. Effect of wall boundary layer suction for triple slotted flap configuration.

2-D optimization results

A large number of parameter variations have been carried out with different leading and trailing edge devices, including single-double and triple slotted flaps in order to optimize each combination of flap elements and also to study the parameter trends (Refs 5 and 6). Fig 5 shows some of the best results in terms of lift and drag for different configurations.

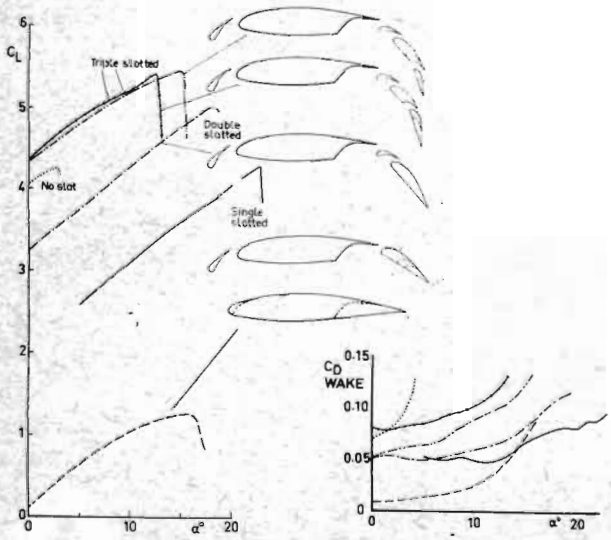

Figure 5. Summary of lift and drag results for different 2-D configurations.

The results from all the parameter variations behind these optimized results have been analyzed in order to get a general idea about the performance trends for different geometrical parameters and the correlations between them. The importance of the interaction between leading edge and trailing edge optimization was one of the most interesting findings.

This can be further explained if we have a closer look at the leading edge slat. Fig 6 shows some results for a variation of slat gap.

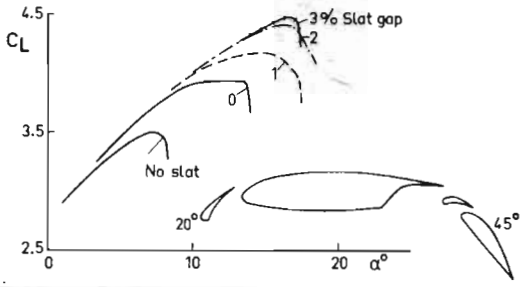

Figure 6. Gap effects for a 20° slat.

The deflection of the slat without any gap gives an improvement due to the modified pressure distribution, which causes a delay of the final leading edge stall. There is however a gradual trailing edge separation prior to the final stall. A slat gap of 1 % has obviously an effect on both the leading edge and the trailing edge separation. A further increase of the slat gap does not influence the leading edge stall, but controls the development of the trailing edge separation. The gap size determines the development and interaction of the slat wake and main wing boundary layers which in its turn controls the characteristics of the viscous wake above the trailing edge flaps.

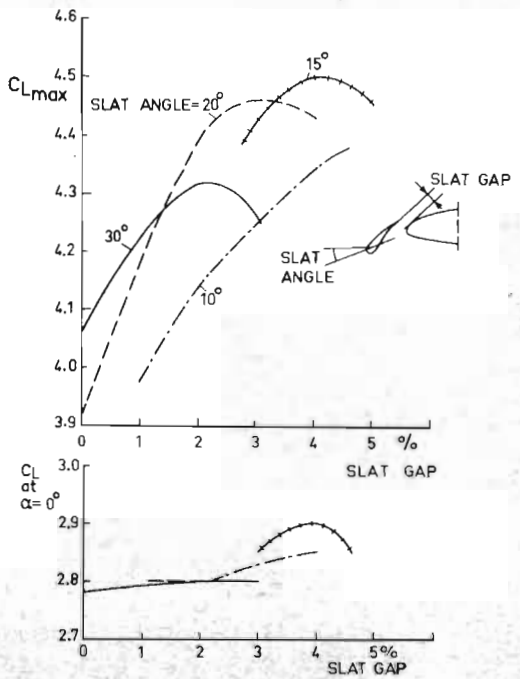

Figure 7. Slat gap effect for different slat angles.

Fig 7 shows $C_{L\ max}$ as a function of slat gap for different slat angles. The optimum slat gap increases with a decreasing slat angle. This is due to the reduced size of the slat wake relative to the main wing boundary layer with increasing slat angle which requires a smaller gap to obtain the optimum viscous interaction. The trends for $\alpha = 0$ should indicate that the potential flow effects are comparatively small. The gap trends are primarily due to viscous effects.

III. Boundary layer study of slat wing-flap interaction

A series of boundary layer measurements were performed with a model according to Fig 8 in order to get a better understanding of the viscous effects discussed above and their relative importance for the optimization trends (Ref 7).

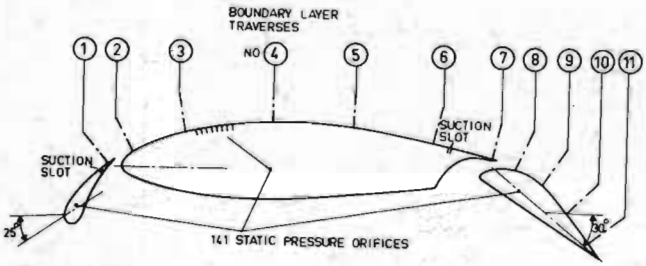

Figure 8. 2-D model for boundary layer experiments.

Slot suction is introduced on this model at the trailing edge of the slat and the main wing element as indicated in the figure. The suction is not for conventional boundary layer control purposes. It is used to reduce the thickness of the wake leaving the trailing edges of the slat and the wing. This will make it possible to vary the conditions for the viscous interaction between the slat wake and the main wing-flap boundary layers, and also between the main wing wake and the flap boundary layer. The position of the slot and the suction quantities are such that the sink effects are an order of magnitude smaller than the observed C_L-differences.

The model was first tested for a number of slat gaps and a fixed slat angle in order to obtain the kind of slat trends that were observed for the experiments discussed above. The slat angle was selected with the assistance of potential flow calculations (Ref 4).

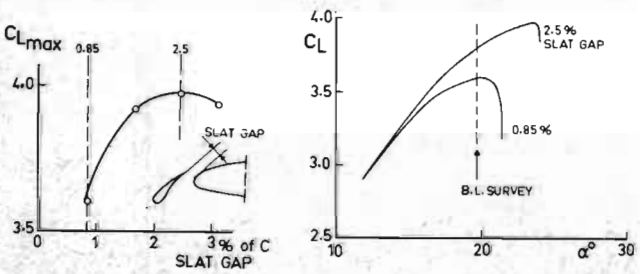

Figure 9. Slat gap effect for 25° slat.

The results as shown in Fig 9 exhibit the familiar slat gap trend with an optimum gap at 2.5 %. This gap and a smaller 0.85 % gap were selected for further studies. Boundary layer total head measurements were performed at eleven stations along the upper surface of the model at an angle of attack which is 1.5° below the stall.

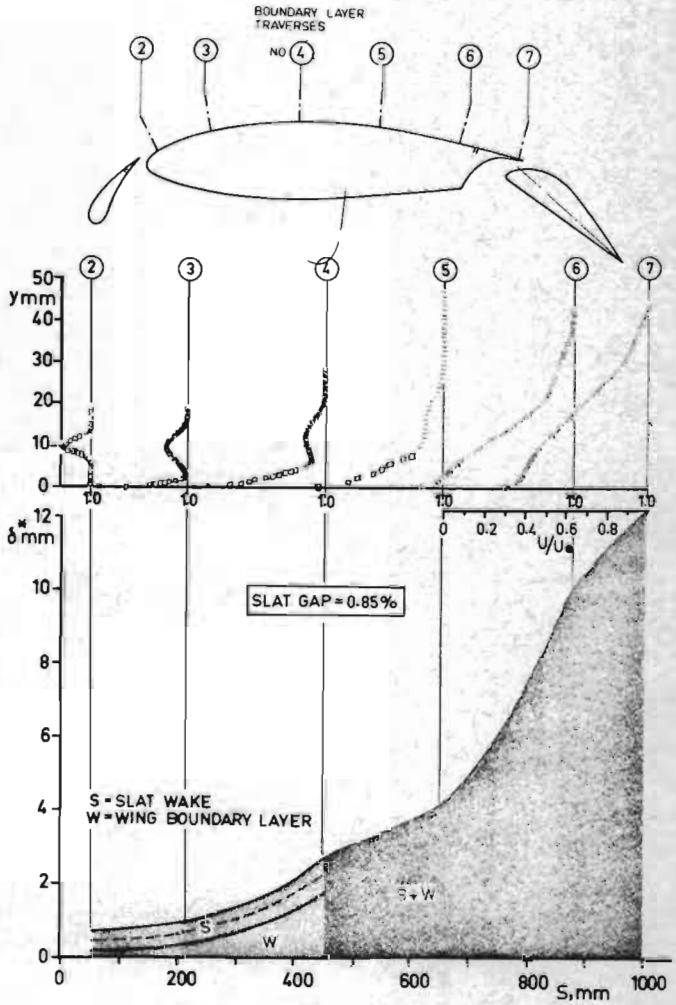

Figure 10. Boundary layer velocity profiles and displacement thickness above wing element for a 0.85% slat gap.

Fig 10 shows velocity profiles and displacement thickness above the main wing surface for the case with a 0.85 % slat gap. The contributions from the slat wake (SW) and the main boundary layer (W) to the total displacement thickness are indicated up to the point where they have merged (somewhere between stations 4 and 5). The corresponding results for the case with the optimum slat gap (2.5 %)are plotted in Fig 11.

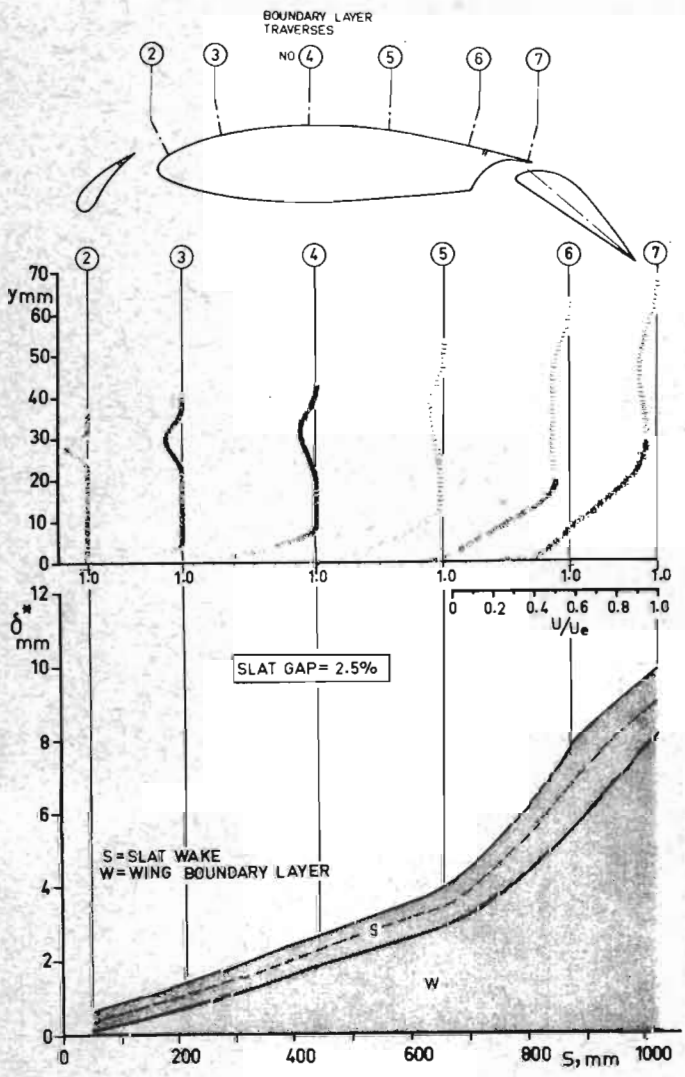

Figure 11. Boundary layer velocity profiles and displacement thickness above wing element for a 2.5% slat gap.

The development here is quite different. The viscous layers do not merge completely over the main wing and the displacement thickness growth over the rear part is less pronounced. The displacement thickness and the shape factor H are compared for the two different slat gaps in Fig 12.

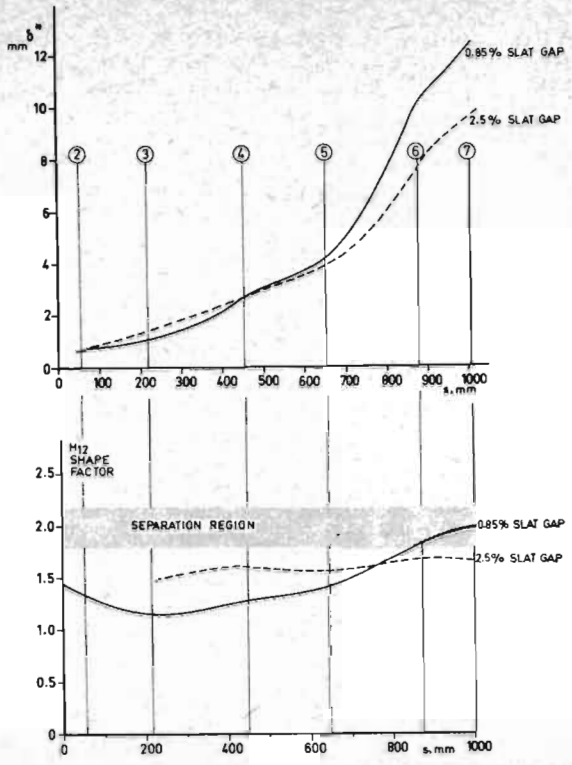

Figure 12. Comparisons of displacement thickness and shape factor on main wing element for two different slat gaps.

The total displacement thickness at station 2 is the same for the two cases but the following development is quite different. The larger gap shows a larger displacement thickness between stations 2 and 4 which is due to the differences in pressure distribution as shown in Fig 13. The following development shows the effects of the interaction between the layers. The small gap case with considerable interaction gives a more rapid growth of displacement thickness resulting in a significant difference at the trailing edge of the main wing. The pressure distributions on this part of the wing are similar enough to outrule any significant contribution to this difference.

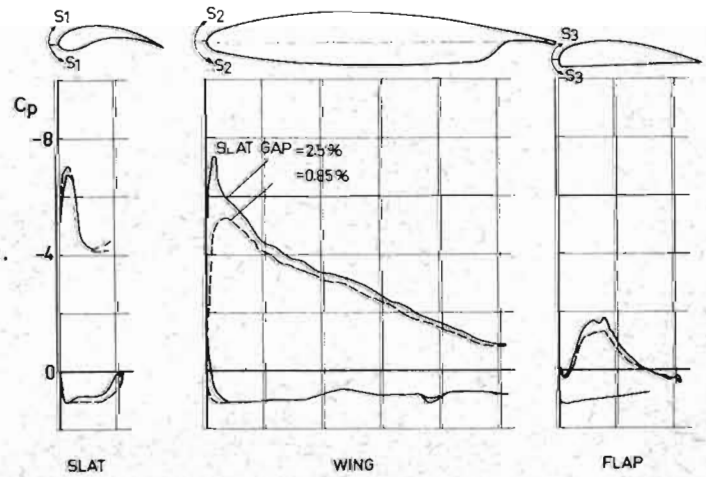

Figure 13. Slat gap effect on pressure distribution. $\alpha = 19.6^{\circ}$.

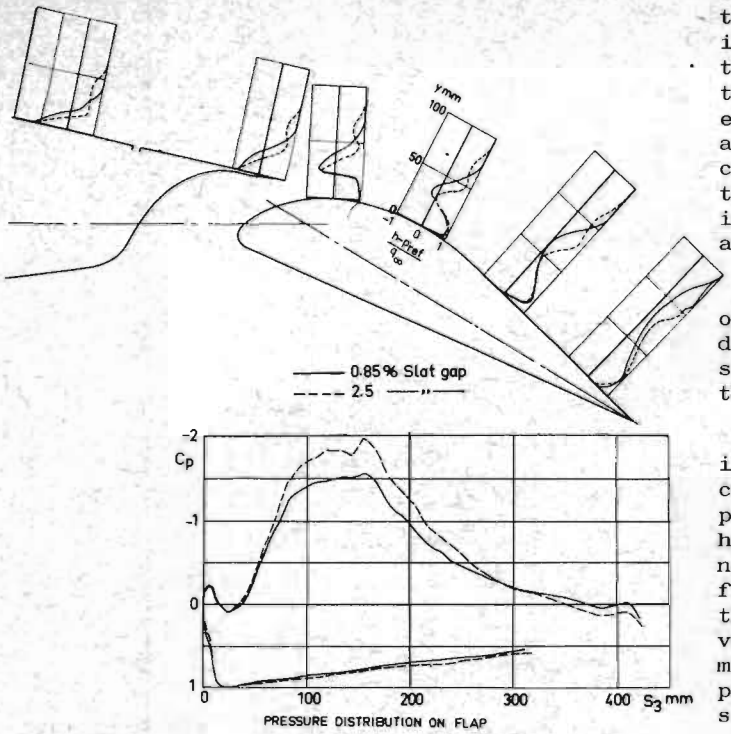

Figure 14. Slat gap effect on total head profiles and pressure distribution for T.E. flap.

Fig 14 shows total head profiles over the trailing edge of the configuration for the two different slat gaps. The viscous development for the 2.5 % gap case as discussed above results in a more efficient flow over the flap. There is a significant difference in the size of the main wing wake at the trailing edge of the flap. The improvement in flow efficiency is further illustrated by the pressure distribution on the flap.

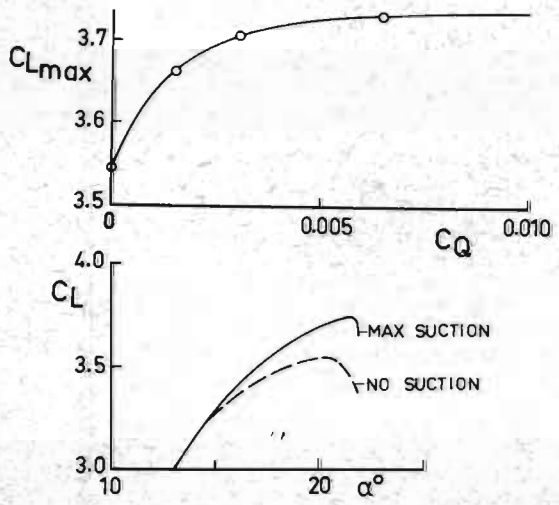

Figure 15. Effect of reduced slat wake on $C_{L\ max}$ and C_L.

The variation of slat gap has been shown to change the conditions for the interaction between different viscous layers. It has however in the same time changed the local pressure distributions at the leading edge of the slat and the main wing element. The effect on the flow efficiency over the flap results from a combination of direct viscous effects due to the changed geometry and indirect effects due to the changed pressure distribution. The question is what exactly is the role of the viscous interaction in these results.

In an attempt to answer this question and others, suction was applied on the slat as indicated in Fig 8, for the case with the smaller slat gap 0.85 %. The effect of this suction on the C_L-results are shown in Fig 15.

The shape of the C_L-alfa curve has changed in a way quite similar to the case for the increased slat gap as shown in Fig 9 with one important difference, the stall angle of attack has not increased. The leading edge stall has not been affected. The $C_{L\ max}$-curve levels off for the highest amounts of suction indicating that the remaining part of the slat wake has very little effect on the separation development. Fig 16 shows velocity profiles and displacement thickness for the case with maximum slat suction, C_{Qs} = 0.0065.

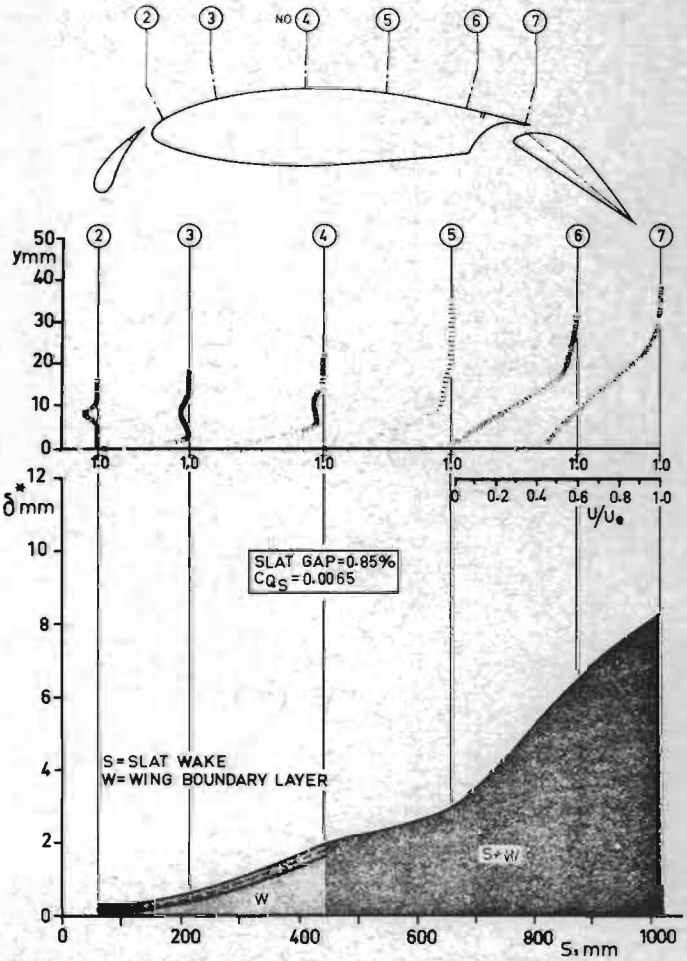

Figure 16. Boundary layer and displacement thickness above main wing element for case with 0.85% slat gap and maximum slat suction C_{Qs}= 0.0065.

The effect of this suction on the slat wake is evident if the wake contribution to the displacement thickness at station 2 is compared to the case with no suction shown in Fig 10.

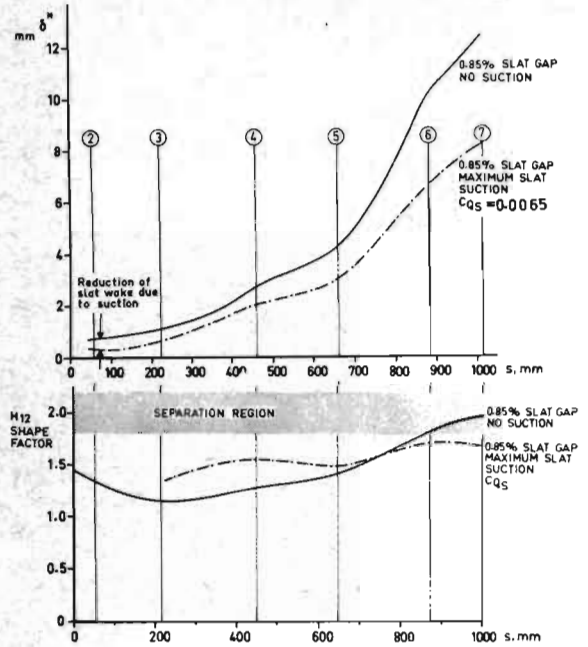

Figure 17. Comparison of displacement thickness and shape factor on main wing wlement för 0.85% slat gap with and without slat suction.

Fig 17 compares displacement thickness and shape factor for the small gap with and without slat suction. The development is quite parallel up to the region where the layers start to interact as shown in Fig 16. After this the curves are no longer parallel but spread apart significantly. The pressure gradient is almost constant from station 2 to station 7 (see Fig 18) and essentially identical for both cases, which means that the potential flow conditions are the same.

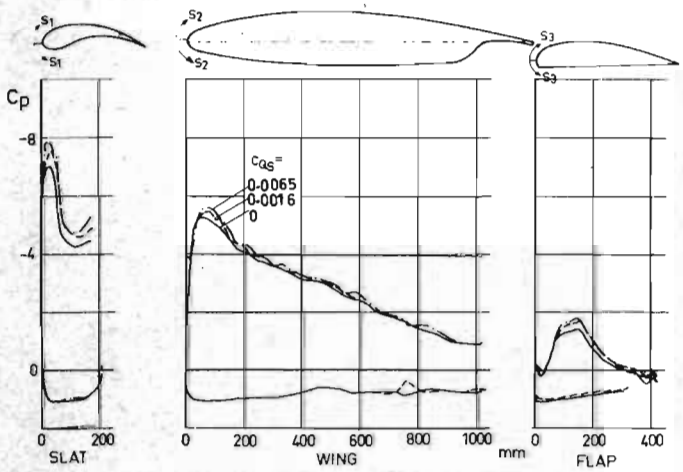

Figure 18. Effect of reduced slat wake on complete pressure distribution.

This seems to indicate that the interaction between the shear layers accounts for a substantial part of the difference in displacement thickness between the two cases.

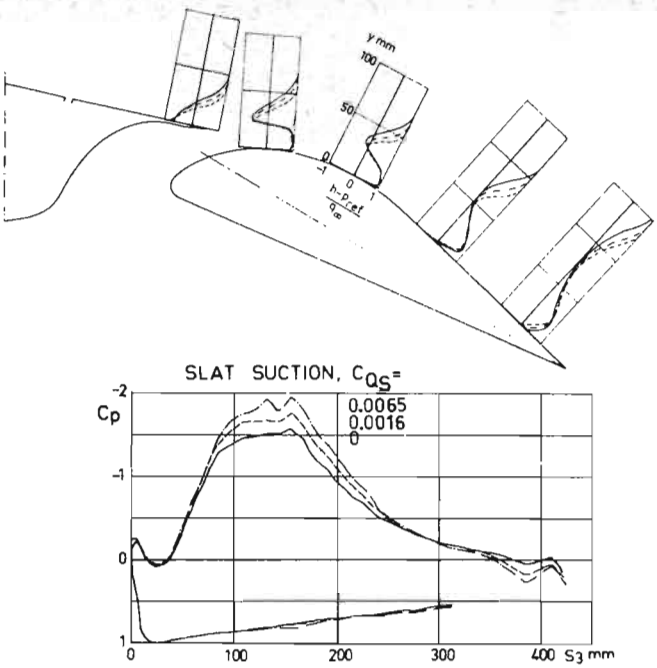

Figure 19. Effect of reduced slat wake on total head profiles and pressure distribution of T.E. slap. α= 19.6°.

Total head profiles over the trailing edge flap for different amounts of suction are compared in Fig 19. The suction effects on the boundary layers at the main wing trailing edge and the flap trailing edge are similar to those for the increased slat gap discussed above. The reduction of the wake over the flap results in improved flap efficiency which is also shown by the pressure distributions on the flap.

One conclusion that can be drawn from this is that the viscous effects over the main wing and the flap due to an increased slat gap are essentially similar to elimination of a major part of the slat wake.

The optimum slat gap corresponds to an optimum amount of mixing between the slat wake and the main wing boundary layer. This is achieved, for the present case, with only marginal interaction between the slat wake and the main wing boundary layer.

This should not be treated as a general result for any slat-airfoil combination. The optimum viscous flow conditions depend strongly on the slat angle as illustrated in Fig 7. A bigger slat angle gives a smaller slat wake resulting in a reduced optimum slat gap.

There are two different reasons for this. The smaller physical size of the slat wake results in a smaller gap for the same amount of interaction. The reduced momentum loss in the slat wake means that more interaction will take place for the optimum position - resulting in a further reduction of the gap.

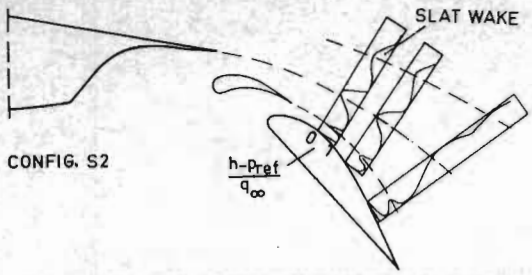

Figure 20. Total head profiles on optimezed double slotted flap.
$\alpha = \alpha_{STALL} - 1.5^{o}$.

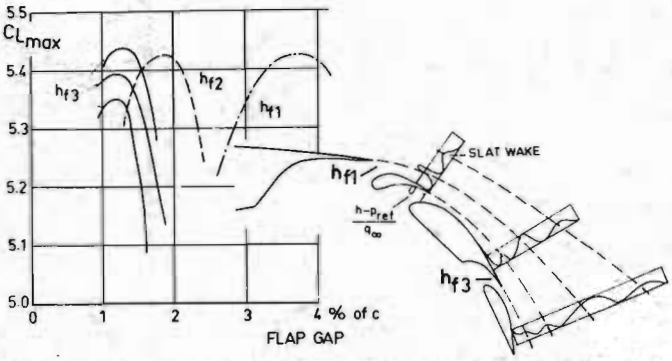

Figure 21. Total head profiles and gap optimization trends for triple slotted flap.

Figs 20 and 21 show some boundary layer traverses that were taken on double and triple-slotted configurations for which a large number of parameter variations have been carried out. The measurements shown are in both cases taken on geometries with the optimum combination of slat and flap positions at an angle of attack 1.5^{o} below the stall.

The slat wakes are in both cases quite distinguishable at the trailing edge of the last flap. The total head profiles for the triple slotted case indicate less interaction between the slat wake and the other shear layers compared to the single slotted configuration discussed above. This can be explained by the smaller slat angle (20^{o} instead of 25^{o}) and the higher lift coefficient (5.4 instead of 3.7) resulting in a more pronounced slat wake. The potential adverse effects of interaction between this wake and other shear layers are greater and it becomes more important to keep the layers apart.

The total head profiles in Figs 20 and 21 also show that similar conclusions can be drawn about the trailing edge gaps. The gaps which give the best $C_{L\ max}$ correspond to a flow where all the different viscous layers over the flap are essentially separated by potential flow cores. They are just beginning to merge at the trailing edge of the last flap. This type of trailing edge condition has occurred for the optimum geometry of all the different configurations tested, including single, double and triple slotted flaps. It is therefore tempting to suggest this condition as a general criterion for $C_{L\ max}$ optimization. It may then be possible to set up some empirical relation between gaps and other parameters which can be used to determine the gap sizes that will satisfy the trailing edge condition!

The optimum size of any gap would then be expressed as a function of the following parameters:

- The size (momentum loss thickness) of the viscous layer leaving the trailing edge immediately ahead of the gap.
- The boundary layer thickness at the trailing edge of the following airfoil element.
- The distance from the gap to the trailing edge of the configuration.
- The average pressure gradient over this distance.

This type of empirical knowledge is not sufficient for a purely computational optimization of a high lift geometry. It should however be very helpful in reducing the size of experimental optimization programs.

2-D drag measurements

It should also be noted that the discussions so far have been concerned primarily with lift performance. The optimization problem becomes more complicated when drag and stability become important criteria as well. Drag measurements have been carried out with a wake rake for most of the configurations discussed above. These results have shown that drag trends are not always in conflict with maximum lift.

The optimization of gaps for a fixed set of flap angles resulted in a geometry which also has nearly minimum drag! The gaps should only be slightly reduced if minimum drag is desired for a given set of flap angles. The low level of viscous interaction required for high $C_{L\ max}$ has also a favourable influence on the drag!

If we compare the lift to drag ratio of different flap configurations we find that it appears to be independent of the C_L-level. All 2-D configurations that have been carefully optimized from single slotted flaps up to triple slotted ones have given L/D-values approaching 100. The 2-D drag measurements therefore do not give any conclusive trends that can be used for the 3-dimensional trade off between $C_{L\ max}$ and L/D, which is particularly important in the take off case.

The drag measurements are however very useful in the 2-D tests, because they will indicate the best possible solution at each $C_{L\ max}$ level. They should be seen as sensitive measurements of the flow efficiency.

The 2-D L/D results can of course be used to calculate potential 3-dimensional performance for different planforms. A number of flap alternatives selected from the 2-D results could then be tested 3-dimensionally and compared to the predictions.

IV. 2-D high lift calculations

The difficulties and costs associated with experimental optimization of high lift devices have stimulated efforts to develop calculation methods that will reduce or eventually even replace the experiments.

The measurements discussed in this paper have shown the importance and complexity of the viscous flow. The ability to handle this theoretically will determine whether a calculation method can be used for optimization purposes.

The potential flow for multiple element airfoils can be calculated with several available methods (Refs 4, 8). The serious difficulties begin when existing boundary layer models are to be introduced into the potential flow. It becomes necessary to predict the growth of all the different boundary layers involved, the growth of wakes shed from different components, the interaction between wakes and boundary layers and the onset of local separations due to these viscous developments. Several quite different approaches to this problem have been tried by different authors. Some of these attempts are commented in the following.

Stephens and Goradia (Ref 8)

Stephens and Goradia at Lockheed have developed a method which uses a vorticity distribution for the potential flow and introduces the displacement effect of interacting viscous layers over the main wing element.

The method assumes attached flow and does not contain a representation of separate wake layers over the main wing and the flap. The interaction effects are introduced into one single displacement thickness which is added to the surface of the airfoil elements. Calculations with this method have been carried out for the single slotted "boundary layer model" shown in Fig 8.

The purpose was to see whether this method could predict the effects of different slat gaps, which should be a good test case for the ability of the method to handle viscous interaction. The calculated pressure distributions for two different slat gaps are compared with corresponding experimental results in Fig 22.

The pressure distribution on the flap is of particular interest. The experiments show this to improve for the bigger slat gap. The calculations show the opposite effect, a reduced flap pressure for the bigger slat gap.

The reason for this is probably that the calculation model for the flow over the flap does not account for a separate wake layer above the flap. The layers are instead combined to one displacement thickness that is added to the flap shape. The calculations show correctly that the increased slat gap causes increased pressure peak at the main wing leading edge. This causes a thicker boundary layer on the main wing which is later added to the flap boundary layer resulting in reduced lift on the flap instead of the improvement obtained for the experiments. Some of the differences may also be explained by local separations for the experiments which cannot be predicted by the calculations.

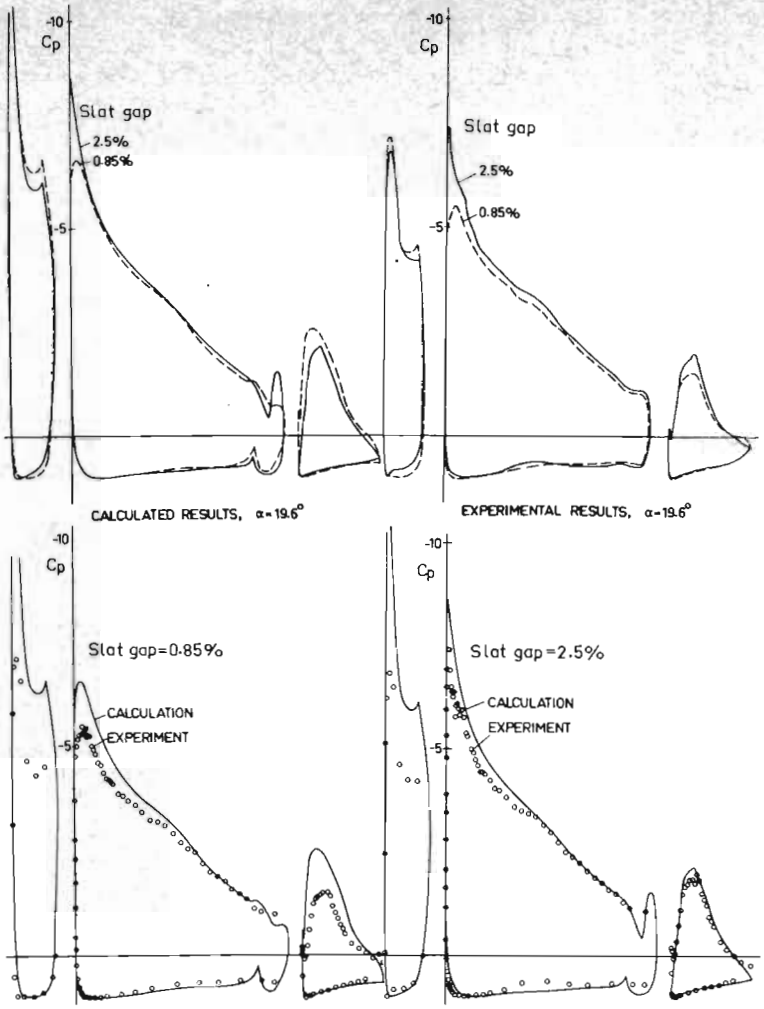

Figure 22. Pressure distributions calculated with Stevens, Goradia method (Ref 8) for two different slat gaps.

The comparisons have shown that the Stephens-Goradia method cannot correctly predict the effects of slat gap variation, due to the discrepancy between the theoretical representation of the viscous flow over the wing and flap and the actual viscous flow as shown by the experimental results.

K. Jacob (Ref 9)

has developed a method for calculation of multiple element airfoils with separation. The displacement thickness of the boundary layer is added to the surface of each airfoil element. A separated region is represented by a source distribution at the trailing edge of one prescribed airfoil element. The separation point is then calculated by an iterative method. The method does not however account for any interaction between different viscous layers. Wakes shed from the trailing edges of the different elements are not represented. It is therefore the authors belief that this method cannot be used to predict separation on highly loaded multiple element airfoils for which viscous interaction and separate wake layers have been shown to have a significant effect on the separation process.

The efforts that appear to be the most promising in terms of the representation of viscous flow effects are those of Foster, Ashill, Williams and Irwin at RAE (Refs 10, 11) and Perrier at Avions Marcel Dassault (Ref 12).

Irwin has developed an integral method for calculation of wake boundary layer interaction. He assumes a power-law boundary layer and an outer gaussian self preserving wake with a pronounced velocity minimum. This model is useful as long as the interaction is relatively weak. The experimental results discussed above have shown that optimum geometries are obtained when the interaction is weak over most of the airfoil surface.

In order to test the validity of the wake representation used in this relatively simple model some comparisons have been made with boundary layer measurements for the model shown in Fig 8.

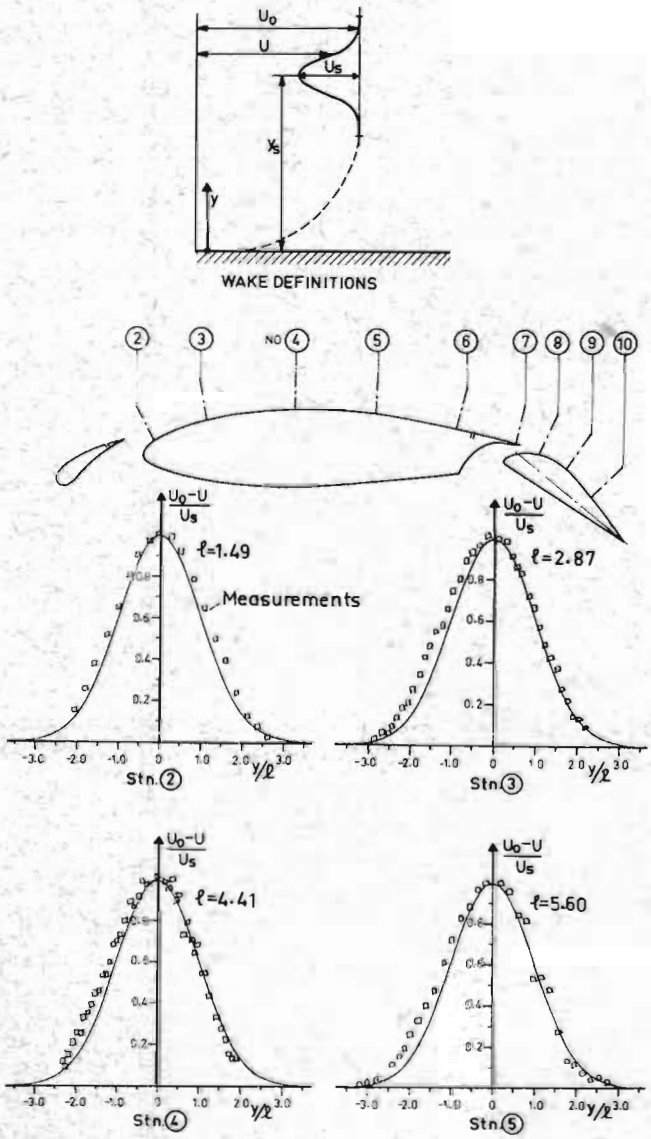

Figure 23. Non dimensional velocity defect profiles for slat wake compared to selfpreserved wake according to Tennekes, Lumley, Ref 13.

Fig 23 shows non dimensional velocity defect profiles of the slat wake for the case with 2.5 % slat gap compared to calculated 2-D self preserved wake (constant pressure, Ref 13). The experimental wakes have been scaled to the same momentum loss thickness θ, using the transverse length scale, ℓ. The general wake shapes seem to agree very well. The variation in ℓ as shown in the figure is only about 15 % greater than the expected variation for a case with constant pressure. It may therefore be possible to introduce the effect of pressure gradient as a variation of the transverse length scale.

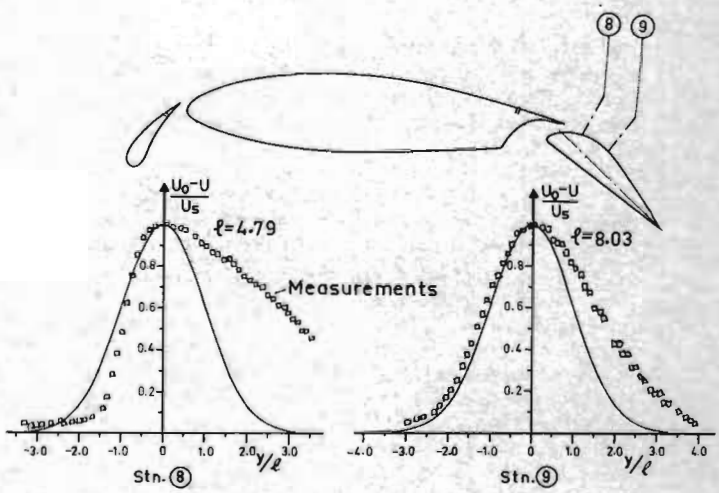

Figure 24. Non dimensional velocity defect profiles for main wing wake compared to selfpreserved wake according to Ref 13.

Fig 24 shows the corresponding plots for the main wing wake above the trailing edge flap. The velocity profile at station # 8 is definitely not of gaussian shape but it seems to approach such a shape quite rapidly as indicated by the situation at station # 9.

It seems reasonable to assume that any wake of interest for a high performance configuration will have reached a shape similar to a self preserving gaussian wake before any significant interaction takes place. This means that such a wake representation should be quite useful for the further development of viscous calculation methods for multiple-element airfoils provided that the proper variation of transverse length scale can be obtained from the pressure distribution.

V. Conclusions

Improved knowledge of flap aerodynamics and careful optimization procedures will make it possible to improve the performance of mechanical flaps, both in terms of lift and drag.

Mechanical flaps will remain a practical cost efficient solution for STOL aircraft operations down to fairly short field lengths. The potential benefits of going from a 3000 ft mechanical flap operation to a 2000 ft powered lift system will not be big enough to justify the increased costs.

The highest maximum lift for a multiple element airfoil is obtained for a geometry where the interaction between all the viscous layers is marginal up to the stall.

Interaction between the slat wake and the main wing boundary layer causes a significant increase of the total displacement thickness compared to the combined displacement thicknesses of two non-interacting layers. The interaction causes premature separation at the trailing edge of the main wing element (as indicated by the shape factor, H) or at the flap trailing edge.

Calculation methods which are to be used for theoretical optimization of a high lift geometry must contain a representation of the various wake regions above the main wing and flaps including the effect of weak to moderate interaction between wakes and boundary layers and its impact on separation.

Experimental wakes with weak interaction have been shown to agree fairly well in shape with a calculated selfpreserved plane wake when scaled to the same momentum loss thickness. It seems possible to use such a relatively simple wake representation in a calculation method if the variation in transverse length scale can be calculated from the pressure distribution.

VI. References

1. Morris, Hanke, Pasley, Rohling — The influence of wing loading on turbofan powered STOL transports with and without externally blown flaps. NASA CR 2320 (Nov 1973)

2. Perrier, P. Lavenant, M. — Progres recents dans l'hypersustentation mecanique. AGARD-CPP-143 (April 1974)

3. Ljungström, B.L.G. — Experimental high lift optimization of multiple element airfoils. AGARD Symposium on V/STOL Aerodynamics, (April 1974)

4. Giesing, J.P. — Solutions of the flow field about one or more airfoils of arbitrary shape in uniform flows by the Douglas-Neumann method. Douglas Aircr.Co. Report LB 31946 (Dec 1965)

5. Ljungström, B.L.G. — Wind tunnel high lift optimization of a multiple element airfoil. FFA Report AU-778

6. Ljungström, B.L.G. — 2-D wind tunnel experiments with double and triple slotted flaps. FFA Technical Note AU-993 (Nov 1973)

7. Ljungström, B.L.G. — Boundary layer studies on a two-dimensional high lift wing. FFA Report AU-862 (Oct 1972)

8. Stevens, W.A. Goradia, S.H. Braden, J.A. — Mathematical model for two dimensional multi-component airfoils in viscous flow. NASA CR-1843 (1971)

9. Jacob, K. Steinbach, D. — A method for prediction of lift for multi-element airfoil systems with separation. AGARD CPP 143 (April 1974)

10. Irwin, H.P.A.H. — A calculation method for the twodimensional turbulent flow over a slotted flap. RAE Technical Report 72124 (ARC 34236) (1972)

11. Foster, D.N. Ashill, P.R. Williams, B.R. — The nature, development and effect of the viscous flow around an aerofoil with high-lift devices. ARC CP No. 1258 (1974)

12. Perrier, P. Deviers, J.J. — Calculs tridimentionnels d'hypersustentation. Avions Marcel Dassault, 8467

13. Tennekes, H. Lumley, J.L. — A first course in turbulence. MIT Press (1974)

D I S C U S S I O N

V.L. Marshall (British Aircraft Corporation, Weybridge, U.K.): Since a potential flow multi-element theory was used to design the slat/wing parting profile, and the presentation has shown the viscous merging of the slat wake/wing boundary layer - would it not be more desirable then to include some viscous effects in the design calculations? This would seem to be particularly important in at least quantifying the size of the slat trailing edge boundary layer.

B.L.G. Ljungstrom: It was pointed out in the presentation that the potential solution referred to in this instance was only employed to determine the required slat angle of 25^{0}, it was not used to determine the slat geometry in advance.

B.G. Newman (McGill University, Montreal, Canada): In theoretical predictions, the inclusion of a wake is difficult when displacement thicknesses are used to simulate viscous effects because there is jump in the δ^{x} slope at the trailing edge and the Kutta condition becomes uncertain. A better method is to simulate boundary layers and wakes using sources placed on the surface and use a Kutta condition in which the velocities at the edge of the boundary layer are made equal.

A. Das (DFVLR - Braunschweig, Germany): You expressed in conclusion that you are concerned with the deviation between the theoretical and experimental results of pressure distributions especially on the rear flap. As we are since long working on the same problems we are well acquainted with this difficulty. There are two sources which cause trouble - one the cavity on the lower side of the main wing and then its wake interference. In the cavity a standing vortex appears and hence modifies the flow of the oncoming wall streamline - the free streamline having almost constant pressure inside the cavity determines the boundary conditions in this region and not the boundary of the curved wall in the cavity. This has significant effect on the closely lying nose area of the rear flap. We are trying some modified boundary conditions in this region. The wake problem gives still certain difficulties to simulate it completely satisfactorily.